Stem Cell Reports
Article

ISSCR

OPEN ACCESS

H3K27me3 Does Not Orchestrate the Expression of Lineage-Specific Markers in hESC-Derived Hepatocytes In Vitro

Jolien Vanhove,[1,5,*] Mariaelena Pistoni,[1,5,*] Marc Welters,[1] Kristel Eggermont,[1] Veerle Vanslembrouck,[1] Nicky Helsen,[1] Ruben Boon,[1] Mustapha Najimi,[2] Etienne Sokal,[2] Philippe Collas,[3] J. Willem Voncken,[4] and Catherine M. Verfaillie[1]

[1]Department Development and Regeneration, Stem Cell Institute, KU Leuven, Leuven 3000, Belgium
[2]Laboratory of Pediatric Hepatology and Cell Therapy, Université Catholique de Louvain, Cliniques St-Luc – Institut de Recherche Expérimentale et Clinique (IREC), Brussels 1200, Belgium
[3]Faculty of Medicine, Department of Molecular Medicine, Institute of Basic Medical Sciences, University of Oslo, Oslo 0372, Norway
[4]Department of Molecular Genetics, Maastricht University Medical Centre, 6229 ER Maastricht, the Netherlands
[5]Co-first author
*Correspondence: jolien.vanhove@med.kuleuven.be (J.V.), mariaelena.pistoni@gmail.com (M.P.)
http://dx.doi.org/10.1016/j.stemcr.2016.06.013

SUMMARY

Although pluripotent stem cells can be differentiated into the hepatocyte lineages, such cells retain an immature phenotype. As the chromatin state of regulatory regions controls spatiotemporal gene expression during development, we evaluated changes in epigenetic histone marks in lineage-specific genes throughout in vitro hepatocyte differentiation from human embryonic stem cells (hESCs). Active acetylation and methylation marks at promoters and enhancers correlated with progressive changes in gene expression. However, repression-associated H3K27me3 marks at these control regions showed an inverse correlation with gene repression during transition from hepatic endoderm to a hepatocyte-like state. Inhibitor of Enhancer of Zeste Homolog 2 (EZH2) reduced H3K27me3 decoration but did not improve hepatocyte maturation. Thus, H3K27me3 at regulatory regions does not regulate transcription and appears dispensable for hepatocyte lineage differentiation of hESCs in vitro.

INTRODUCTION

Human embryonic stem cells (hESCs) and induced pluripotent stem cells (hiPSCs) are a renewable cell source for the generation of human hepatocytes that could be used for drug toxicity and metabolization studies (Baxter et al., 2010; Mann, 2015; Ulvestad et al., 2013; Zhang et al., 2013; Zhu and Huangfu, 2013). Although many groups (Baxter et al., 2015; Chen et al., 2012; Godoy et al., 2015; Hannan et al., 2013; Shan et al., 2013; Siller et al., 2015; Ulvestad et al., 2013), including ours (Helsen et al., 2016; Roelandt et al., 2012), have generated pluripotent stem cell (PSC)-derived progeny displaying hepatocyte characteristics, these cells are more akin to fetal than post-natal hepatocytes, and are therefore often termed hepatocyte-like cells (HLCs). For instance, HLCs continued to express α-fetoprotein (AFP), a typical fetal hepatocyte marker (Schmelzer et al., 2006).

At the molecular level, cell fate is controlled by epigenetic mechanisms that modulate chromatin structure and thereby control utilization of genetic information (Boland et al., 2014; Meissner, 2010). Changes in chromatin structure are, in part, induced by specific post-translational modifications of nucleosomal and non-nucleosomal histones (Bannister and Kouzarides, 2011; Harshman et al., 2013). Gene activity has been linked to high levels of tri- and dimethylation of histone 3 lysine 4 (H3K4me3/me2) together with binding of RNA polymerase II (POL2RA) at transcriptional start sites (Pokholok et al., 2005; Schneider et al., 2004; Schubeler et al., 2004). However, H3K4me3 promoter marking by itself does not predict transcriptional activity (Guenther et al., 2007). In hESCs, for instance, promoters of key developmental control genes are marked with both H3K4me3 and repression-associated histone 3 lysine 27 trimethylation (H3K27me3), resulting in a low transcriptional activity status (Azuara et al., 2006; Bernstein et al., 2006; Mikkelsen et al., 2007).

In addition to promoters, enhancers play a critical role in the regulation of tissue-specific gene expression (Heintzman et al., 2009; Ong and Corces, 2012; Wamstad et al., 2012). Enhancer elements are typically located in relatively "accessible" chromatin, i.e., hypersensitive to DNase digestion, often coincide with CpG-poor regions, and act in concert with non-coding RNAs to co-regulate gene expression (Boland et al., 2014; Calo and Wysocka, 2013; Heintzman et al., 2007; Lam et al., 2014; Rada-Iglesias et al., 2011; Stadler et al., 2011; Xie et al., 2013b). Although enhancers are typically decorated with mono-methylated H3K4 marking (H3K4me1), only a fraction of H3K4me1-marked elements are engaged in transcription in a tissue-specific manner (Boland et al., 2014; Calo and Wysocka, 2013; Creyghton et al., 2010; Heintzman et al., 2009; Rada-Iglesias et al., 2011; Visel et al., 2009). In hESCs, poised enhancers harbor H3K4me1 and H3K27me3, while active enhancers are co-marked by H3K4me1 and acetylation of histone 3 lysine

CrossMark
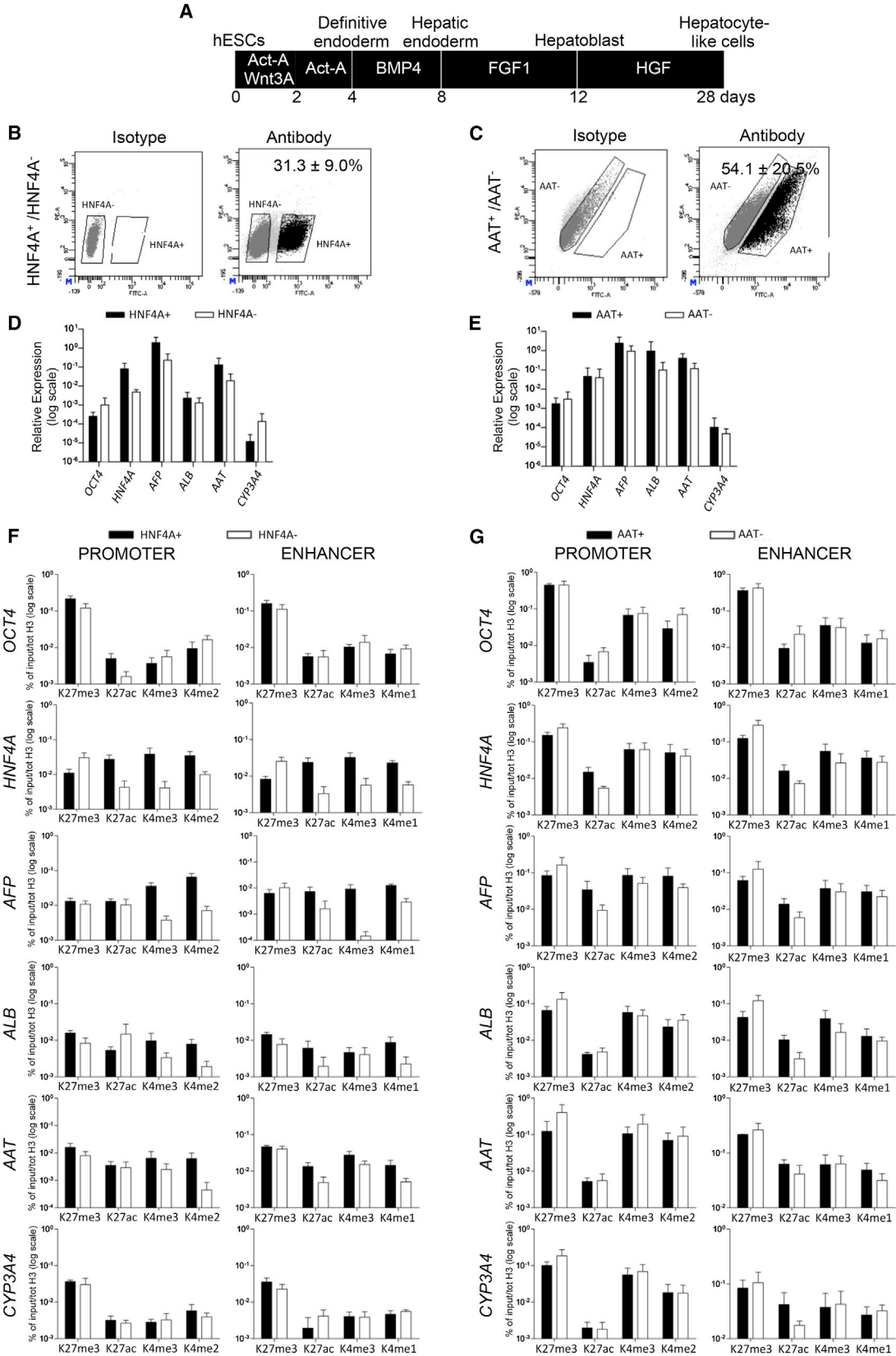
(legend on next page)

27 (H3K27ac) (Calo and Wysocka, 2013; Creyghton et al., 2010; Pekowska et al., 2011).

We hypothesized that mapping histone modifications at promoter and enhancer regions of key pluripotency, hepatic endoderm, and hepatocyte marker genes is likely to provide invaluable information regarding the relevance of epigenetic marking at such regulatory regions during the in vitro hESC-hepatocyte differentiation process that could be used to improve such differentiation protocols. Although a growing number of studies has addressed epigenetic regulation in other cellular contexts, such as for instance β cells (Xie et al., 2013a), neuronal cells (Mikkelsen et al., 2007), or cardiomyocytes (Wamstad et al., 2012), to our knowledge, thus far only one study has been published wherein histone modifications at promoters in the context of hepatocyte differentiation were mapped (Kim et al., 2011).

Here, we examined epigenetic markings in undifferentiated hESCs, hepatocyte nuclear factor α (HNF4A$^+$)-enriched hepatic endoderm cells (HECs), and α1-antitrypsin (AAT$^+$)-enriched HLCs. We also compared the epigenetic status of AAT$^+$ HLCs with uncultured primary human hepatocytes (PHHs). Our studies provide important insights into epigenetic changes that accompany hepatocyte lineage commitment in vitro, and are expected to contribute to the advancement of in vitro generation of mature functional hepatocytes from stem cells.

RESULTS

Alterations in Histone Profile Correlate with Dynamic Changes in Gene Transcription

To address dynamic changes of histone modifications during hepatocyte commitment of hESCs in vitro, we compared histone profiles at promoter and enhancer regions of a selected number of pluripotency, hepatic endoderm, and hepatocyte marker gene specific loci in hESCs, HECs, and HLCs (Figure 1A). As day-8 HECs (d8-HECs) and d28-HLCs represent mixed cell populations, we isolated HNF4A$^+$ cells (31.3% ± 9.0% of d8-hESC progeny) and AAT$^+$ cells (54.1% ± 20.5% of d28-hESC progeny) by fluorescence-activated cell sorting (FACS) to be able to study more homogeneous hepatocyte precursor popula-

tions (Figures 1B, 1C, S1A, and S1B). qRT-PCR confirmed the enrichment for transcripts of the selected lineage-specific marker genes in the d8-HNF4A$^+$ or d28-AAT$^+$ cell populations compared with the d8-HNF4A$^-$ or d28-AAT$^-$ cells, respectively (Figures 1D and 1E). To correlate gene expression with a specific histone profile, we analyzed the enrichment of known active (H3K4me3, H3K4me2, H3K4me1 and H3K27ac) and repressive (H3K27me3) histone marks at promoters and enhancers of the same lineage-specific marker genes by chromatin immunoprecipitation (ChIP)-qPCR in the sorted HNF4A$^+$/HNF4A$^-$ and AAT$^+$/AAT$^-$ populations (Figures 1F and 1G). To demonstrate the effectiveness and validity of the ChIP-qPCR approach, we first analyzed the histone profile at the promoter region of *GAPDH*, a housekeeping gene expressed throughout differentiation. As expected, the promoter region was preferentially decorated with H3K4me3/me2 in all cell populations assessed. In contrast, promoters of *MYOD1* and *HOXD11*, not active in hESCs, HECs, or HLCs, were marked with H3K27me3 (Figures S1C and S1D).

To investigate the relationship between the expression of the different genes and subsequently also histone enrichment, we performed mediation analysis on the d8-HNF4A$^{+/-}$ cells (Krull and MacKinnon, 1999). This demonstrated that gene expression, averaged over all genes, was 2.8-fold higher (95% confidence interval [CI] 78-fold decrease to 35-fold increase) in the HNF4A$^+$ compared with HNF4A$^-$ cells (Figure S1E), confirming the enrichment by FACS sorting. In line with our expectations, the higher transcript levels in the HNF4A$^+$ cells were positively correlated with higher enrichment for all active marks (H3K4me3/me2/me1 and H3K27ac) and inversely correlated with H3K27me3 markings at both regulatory regions (Figures 1D and S1E). Thus, these data indicate that changes in transcription correlate with the alterations observed at the histone profile.

H3K27me3 in the Regulatory Regions of Mature Hepatocyte Genes of d28-AAT$^+$ HLCs May Prevent Differentiation to Mature Hepatocytes

We next compared the gene expression and histone profiles at promoters and enhancers of selected hepatic marker genes throughout differentiation (Figures 2A–2E). We also

Figure 1. hESC-Derived Hepatic Lineage: Two Stages of Lineage Specification Can Be Enriched
(A) Schematic overview of the hepatocyte differentiation protocol.
(B and C) Representative FACS sorting plots for HNF4A on day 8 (B) and AAT on day 28 (C) (right panels) and corresponding isotype controls (left panels).
(D and E) Relative expression (to *GAPDH*) of *OCT4*, *HNF4A*, *AFP*, *ALB*, *AAT*, and *CYP3A4* in sorted d8-HNF4A$^+$ (black)/HNF4A$^-$ (white) cells (D) and d28-AAT$^+$ (black)/AAT$^-$ (white) cells (E).
(F and G) Enrichment of H3K4me3/me2/me1, H3K27ac, and H3K27me3 histone marks at promoters (left panels) and enhancers (right panels) of selected genes in d8-HNF4A$^+$ (black)/HNF4A$^-$(white) (F) and d28-AAT$^+$ (black)/AAT$^-$ (white) cells (G).
Data represent mean ± SEM of n ≥ 3 independent experiments. See also Figure S1.
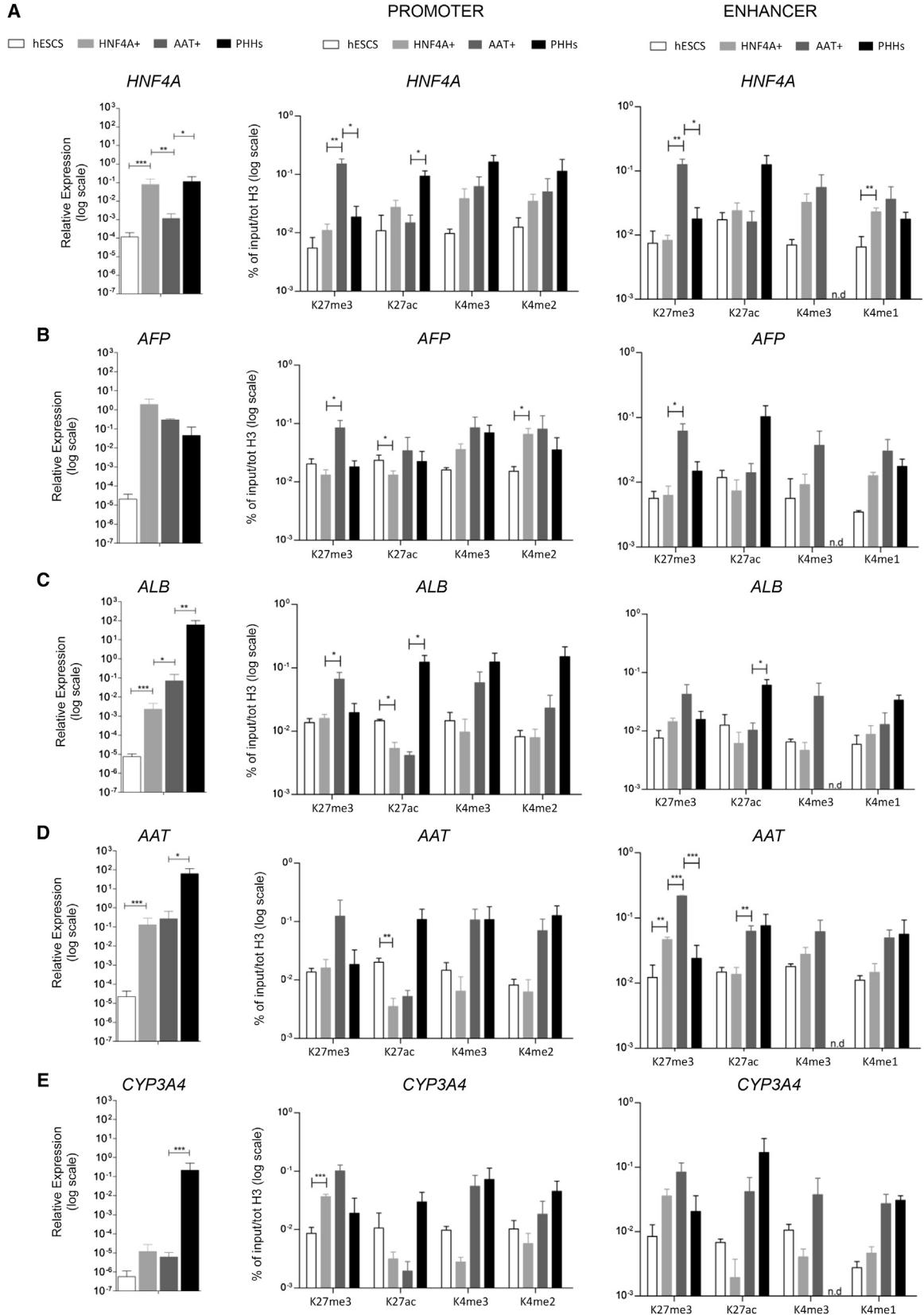
(legend on next page)

compared the gene expression and histone profile in d28-AAT+ sorted cells with PHHs, as this potentially provides important information with which to optimize differentiation protocols (Figures 2A–2E).

As expected, nucleosomes at the *GAPDH* promoter in hESCs, d8-HNF4A+, and d28-AAT+ cells and PHHs were preferentially marked with H3K4me3/2, while *MYOD1* and *HOXD11* promoters were marked with H3K27me3 (Figures S2A and S2B).

Transcripts of the transcription factor (TF) *HNF4A*, which regulates expression of several hepatocyte genes and plays a critical role in liver development, were most highly expressed in d8-HNF4A+ cells, at levels similar to those in PHHs. Levels of H3K27me3 at the *HNF4A* promoter and enhancer of d8-HNF4A+ cells and PHHs were similar, while active marks (especially H3K27ac; enhancer) were slightly higher in PHHs than in d8-HNF4A+ cells (Figure 2A). The lower *HNF4A* transcript levels in d28-AAT+ compared with d8-HNF4A+ cells correlated with increased H3K27me3 at the *HNF4A* promoter and enhancer, while levels of H3K4me3/2/1 and H3K27ac were comparable in both cell populations (Figure 2A).

Transcripts for *AFP*, a typical fetal plasma protein, were highest in d8-HNF4A+ cells and lower d28-AAT+ cells and PHHs. As observed for *HNF4A*, a slight increase in active marks at both the *AFP* promoter and enhancer was observed in d8-HNFA+ cells compared with hESCs, whereas H3K27me3 levels remained relatively low (Figure 2B). Increased H3K27me3 at *AFP* promoter/enhancer regions in d28-AAT+ cells accompanied reduced *AFP* expression, while active marks remained unchanged (Figure 2B). Of note, H3K27me3 levels at the *AFP* promoter/enhancer regions in PHHs were even lower than in d28-AAT+ cells, even though the expression was lower in PHHs compared with d28-AAT+ cells (Figure 2B).

Transcripts of *ALB*, an important serum protein synthesized by the liver, were significantly induced throughout differentiation (Figure 2C). No changes in repressive and active marking at the *ALB* promoter and enhancer were seen between hESCs and d8-HNF4A+ cells. As expected, active marks (H3K4me3 but not H3K27ac) at the *ALB* enhancer and promoter were higher in d28-AAT+ than in d8-HNF4A+ cells. Unexpectedly, higher levels of H3K27me3 were found at the pro-

moter and enhancer of *ALB* in 28-AAT+ compared with d8-HNF4A+ cells (Figure 2C).

Transcripts for *AAT*, another serum protein synthesized by the liver, were also significantly induced throughout differentiation (Figure 2D). In hESCs and d8-HNF4A+ cells, active and repressive marks at the *AAT* promoter and enhancer were low (Figure 2D). Compared with d8-HNF4A+ cells, in d28-AAT+ cells the *AAT* promoter was highly enriched for H3K4me3/2 but not H3K27ac, and the *AAT* enhancer also contained more active marks (H3K27ac and H3K4me3). However, similar to the *ALB* regulatory regions, H3K27me3 at the *AAT* promoter/ enhancer was significantly higher in d28-AAT+ than in d8-HNF4A+ cells (Figure 2D). Enrichment for active marks at the promoter and enhancer of *AAT* d28-AAT+ cells and PHHs appeared to correlate best with increased expression, whereby histone methylation was more prominent at the *AAT* promoter, and histone acetylation at its enhancer. Again, H3K27me3 marking did not correlate with transcriptional activity.

In line with the fact that HLCs remain immature, transcript levels of *CYP3A4*, responsible for metabolization of ±50% of drugs, were very low in d28-AAT+ cells compared with PHHs. In PHHs, an active chromatin status of the *CYP3A4* promoter and enhancer was seen (Figure 2E). In d28-AAT+ HLCs, active marks in the *CYP3A4* promoter and enhancer were not significantly different from PHHs. However, levels of H3K27me3 were higher in d28-AAT+ cells compared with PHHs (Figure 2E).

Comparing d28-AAT+ cells and PHHs demonstrated that transcript levels for all lineage-specific genes were 95 times lower (95% CI 62–99) in hESC-derived HLCs compared with PHHs, confirming the immaturity of the HLCs derived in vitro (Figure S2D) (Baxter et al., 2015; Godoy et al., 2015). Furthermore, we found that lower expression levels in d28-AAT+ cells were associated with higher H3K27me3 and lower active marking at both promoters and enhancers of all marker genes tested when compared with the PHHs (Figure S2D). This suggests that inducing a more active histone profile will be necessary to create more mature hESC-derived HLCs in vitro.

Thus, we observed a good correlation between transcriptional activity and active marks at the regulatory regions of hepatic endoderm, and early and more mature hepatocyte

Figure 2. Gene Expression and Histone Modifications in Promoters and Enhancers of Hepatic Marker Genes in hESCs, d8-HNF4A+ Cells, d28-AAT+ Cells, and PHHs

Relative gene expression (to *GAPDH*) (left panels) and epigenetic patterns of H3K4me3/me2/me1, H3K27ac, and H3K27me3 histone modifications at the promoter (middle panels) and enhancer (right panels) of hepatic *HNF4A* (A), *AFP* (B), *ALB* (C), *AAT* (D), and *CYP3A4* (E) genes in hESCs (white), d8-HNF4A+ cells (light gray), d28-AAT+ cells (dark gray), and PHHs (black).

Data represent mean ± SEM of n ≥ 3 independent experiments. *p < 0.05, **p < 0.01, ***p < 0.001 by Student's t test. Note that both gene expression and histone enrichment for d8-HNF4A+ and d28-AAT+ cells represented are identical to the HNF4A+ and AAT+ data in Figure 1. See also Figure S2.
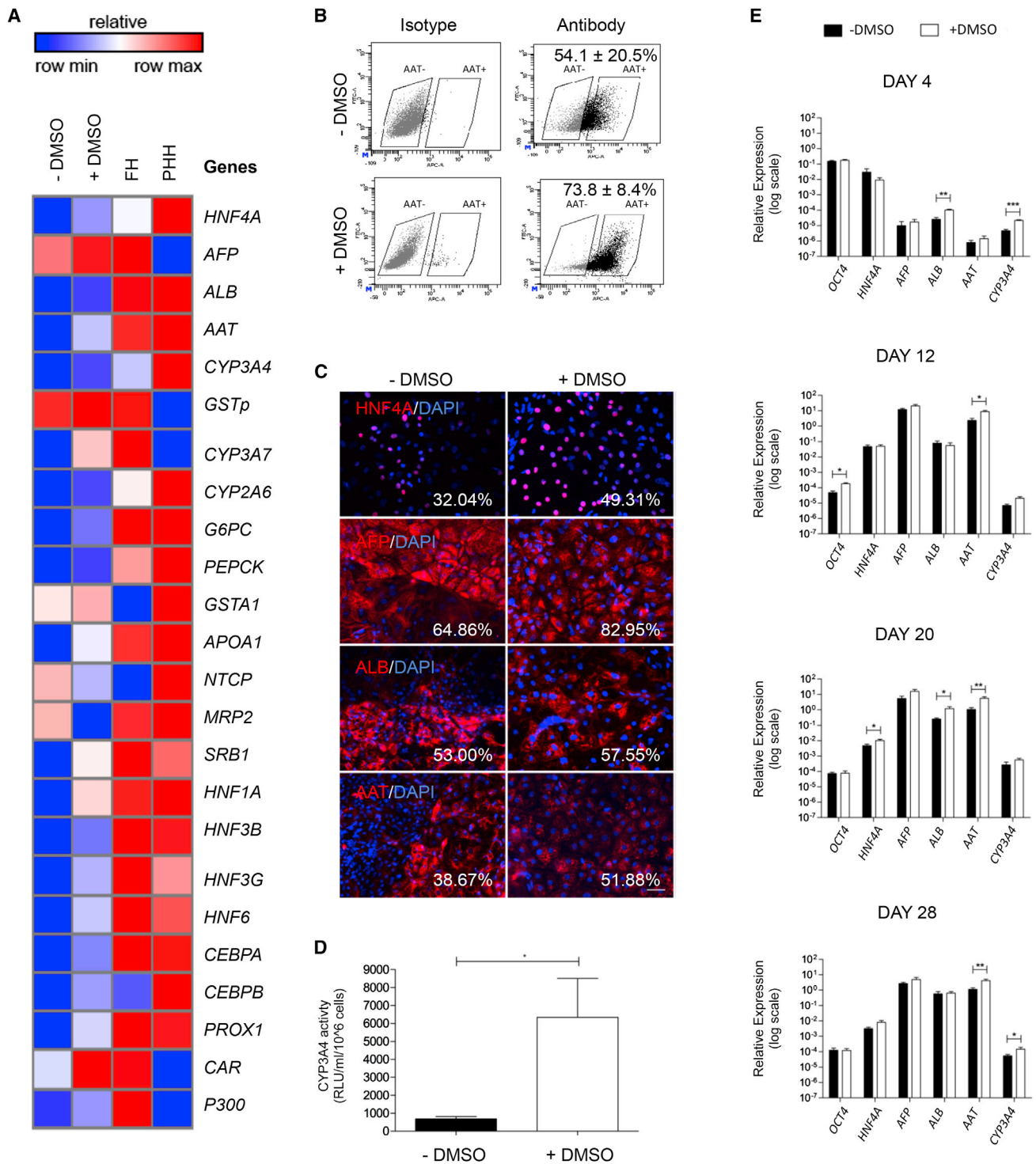
Figure 3. mRNA Transcript, Protein Levels, and Functional Analysis of hESC-Derived HLCs Treated with or without DMSO

(A) Relative gene expression (to *GAPDH*, log scale) analysis represented in a heatmap of pluripotent, fetal hepatic, mature hepatic, drug transporter, and hepatic TF marker genes in cells treated with or without DMSO, FHs, and PHHs.

(B) Representative FACS plots for AAT (right panels) and isotype controls (left panels) on d28-hESC-derived HLCs obtained in the presence or absence of DMSO.

(legend continued on next page)

marker genes in hESCs, d8-HNF4A^{+} cells, d28-AAT^{+} cells, and PHHs. However, higher H3K27me3 marks at promoters and enhancers of *ALB*, *AAT*, and *CYP3A4* in d28-AAT[+] compared with d8-HNF4A^{+} cells did not correlate with the higher transcript levels for *ALB* and *AAT* in d28-AAT^{+} cells. Immunoblotting confirmed the global increase in cellular H3K27me3 in d28-AAT[+] compared with d8-HNF4A^{+} cells (Figure S2C). Of note, PHHs expressed significantly higher levels of all hepatic marker genes compared with d28-AAT^{+} cells, which correlated with higher active and lower inhibitory marks at both regulatory regions. Thus, the continued presence of H3K27me3 at regulatory regions of hepatocyte genes during in vitro differentiation may be responsible for suboptimal maturation of HLCs, suggesting that removal of this mark might be needed to attain full HLC maturation.

DMSO Improves hESC-Derived HLC Homogeneity, but Not HLC Maturation, with Persistent H3K27me3 on Regulatory Regions of Hepatocyte Marker Genes

As DMSO may improve differentiation of stem cell-derived hepatocytes (Basma et al., 2009; Czysz et al., 2015; Duan et al., 2010; Hay et al., 2008; Kanebratt and Andersson, 2008; Kondo et al., 2014; Szkolnicka et al., 2014; Ulvestad et al., 2013), we reassessed histone modifications at regulatory regions of hESC progeny from cultures containing DMSO. Addition of 0.6% DMSO throughout the differentiation protocol resulted in increased expression of the mature hepatocyte genes *AAT*, *CYP3A4*, *CYP2A6*, *G6PC*, *PEPCK*, and *APOA1*, and the mature hepatocyte TFs *HNF3B*, *HNF3G*, *CEBPA*, and *PROX1* on day 28 (Figure 3A). Nevertheless, the expression profile of a broad panel of fetal markers (*AFP*, *CYP3A7*, and *GSTp*) and mature hepatocyte TFs, genes, and drug transporters of d28-HLCs from DMSO-treated cultures resembled fetal, not mature hepatocytes (Figure 3A), in line with other publications (Baxter et al., 2015; Chen et al., 2012; Godoy et al., 2015; Hannan et al., 2013; Shan et al., 2013; Siller et al., 2015; Ulvestad et al., 2013).

In d28-HLCs, the yield of AAT[+] and HNF4A^{+} cells is ±70% and ±50%, respectively, compared with ±50% AAT^{+} cells and ±30% HNF4A^{+} cells in HLCs from cultures without DMSO (Figures 3B and 3C). Addition of DMSO also significantly enhanced CYP3A4 activity by 8- to 10-fold (Figure 3D). To gain insights into the mechanism underlying

the increased frequency of HNF4A^{+} and AAT^{+} cells on days 8 and 28, respectively, and the increased expression of hepatocyte markers in DMSO-treated cultures, we followed the expression of *OCT4*, *HNF4A*, *AFP*, *ALB*, *AAT*, and *CYP3A4* throughout differentiation in the presence or absence of DMSO. Improved expression of hepatocyte transcripts in response to DMSO was only seen on days 20 and 28 (Figure 3E).

We next isolated AAT^{+} cells from DMSO-treated cultures on day 28, and compared their expression profile with AAT^{+} cells from cultures without DMSO. Transcript levels for nearly all genes tested were not statistically different (Figure 4C). Thus, DMSO did not appear to enhance the maturation of HLCs. However, qRT-PCR (Figure S3B) and FACS/immunocytochemistry (ICC) analysis (Figures S3C and S3D) on d4-progeny demonstrated that DMSO significantly increased the fraction of definitive endoderm cells (CXCR4^{+}/C-kit[+] and SOX17^{+} cells), which might be responsible for the increased homogeneity of d28-HLCs.

We compared the gene expression and epigenetic marks for *OCT4*, *HNF4A*, *AFP*, *ALB*, *AAT*, and *CYP3A4* in d8-HNF4A^{+} and d28-AAT[+] enriched populations from DMSO-treated cultures, with results obtained in the absence of DMSO (Figures 1 and 2). Differences in transcript levels were not detected in d8-HNF4A^{+} cells from cultures with or without DMSO (Figure 4A) and not in H3K27me3 marks at promoters and enhancers of the hepatic marker genes. A moderate increase in H3K27ac and H3K4me2/1 (not H3K4me3) marking was observed in DMSO-treated HNF4A^{+} cells (Figure 4B). Consistent with the results obtained for d8-HNF4A^{+} cells, in DMSO-treated d28-AAT^{+} cells neither transcript levels (Figure 4C) nor H3K27me3 enrichment at promoters and enhancers of *ALB*, *AAT*, and *CYP3A4* (Figure 4D) were altered compared with d28-AAT^{+} cells from cultures without DMSO. This further indicates that DMSO does not enhance HLC maturation. Moreover, global H3K27me3 levels were higher in d28-DMSO-treated cells (Figure S4C). Interestingly, total H3 levels were lower in d28-AAT^{+} cells differentiated in the presence of DMSO (Figures S4A and S4B). In addition, H3K27ac and H3K4me3/2 appeared to be lower at the regulatory regions of *ALB*, *AAT*, and *CYP3A4* of d28-AAT^{+} cells derived from cultures with DMSO (Figure 4D). However, we detected an increased presence of POL2RA at nearly all

(C) Representative immunofluorescence images for HNF4A, AFP, ALB, AAT (magnification 20×; scale bar, 50 μm) on day 20 for cells treated without or with DMSO.

(D) Functional CYP3A4 activity in non-treated (black) or DMSO-treated (white) HLCs.

(E) Relative gene expression (to *GAPDH*) for *OCT4* and hepatic markers at different time points (days 4, 12, 20, and 28) of differentiation with (white) or without (black) DMSO.

Data, except for (C), represent mean ± SEM of n ≥ 3 independent experiments. *p < 0.05, **p < 0.01, ***p < 0.001 by Student's t test. See also Figure S3.
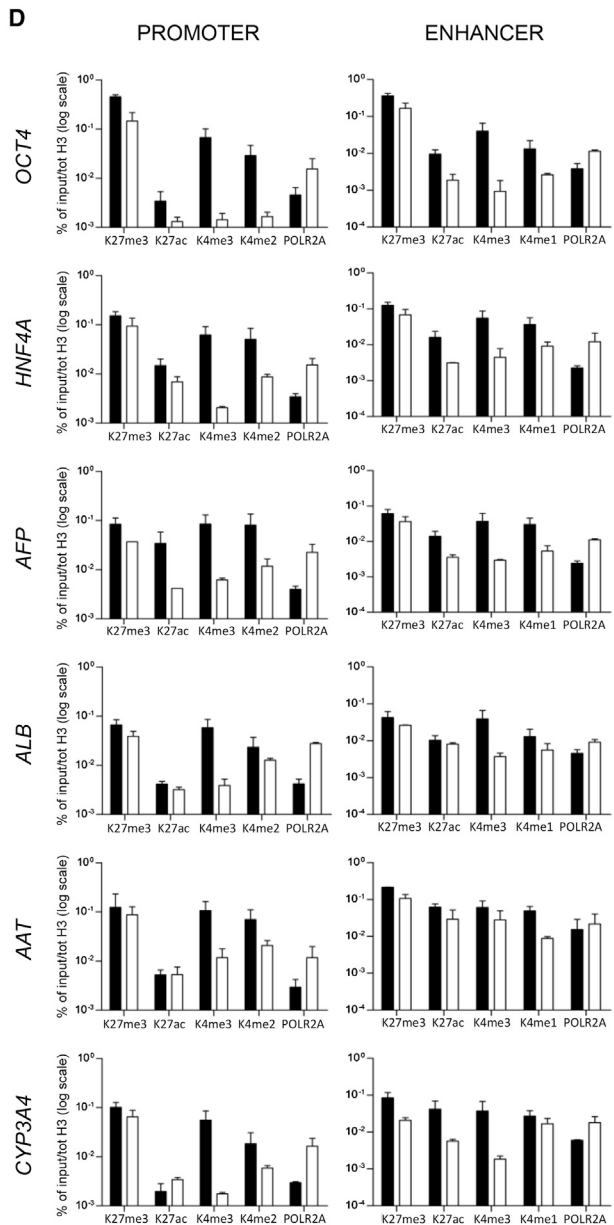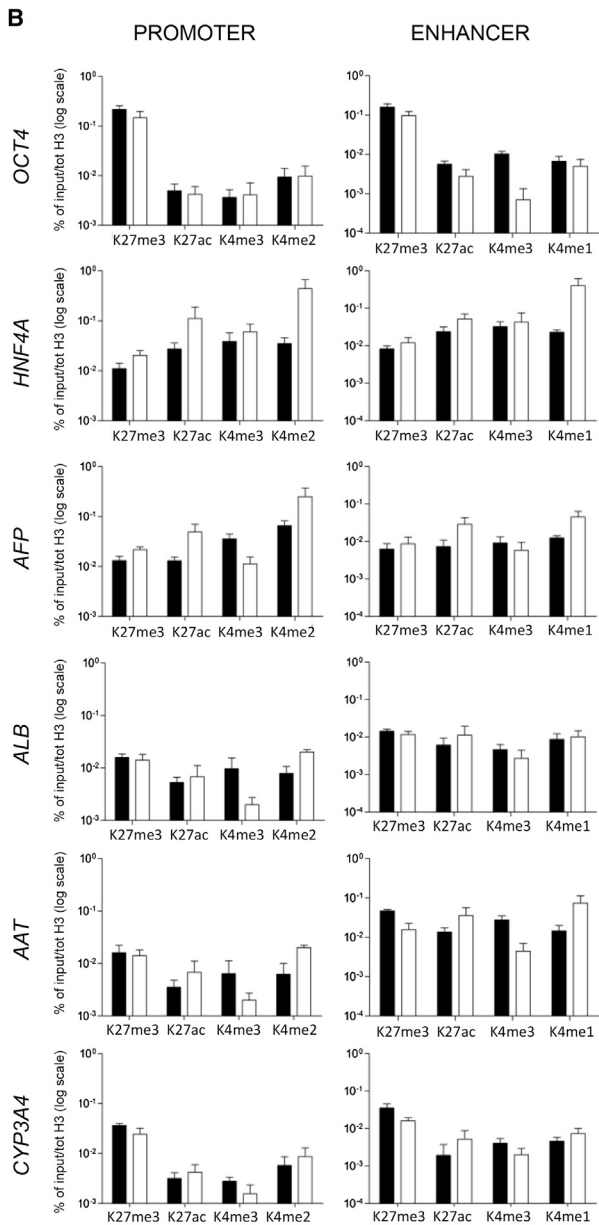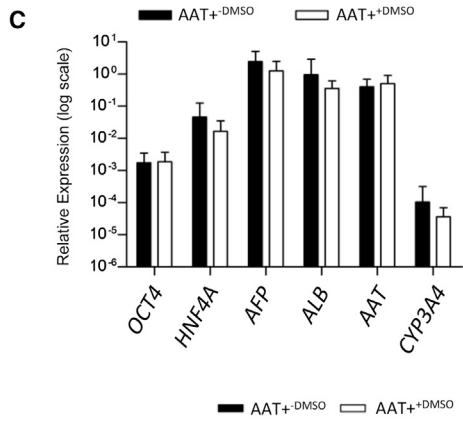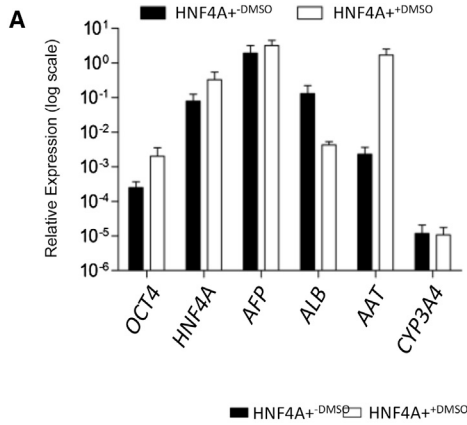
(legend on next page)

gene promoters and enhancers in AAT+ cells derived from DMSO cultures (Figure 4D).

Thus, addition of DMSO during hepatocyte differentiation improved commitment to definitive endoderm, which correlated with a more homogeneous population of d28-AAT+ HLCs. However, none of the transcripts and epigenetic marks at the promoter and enhancer of immature and mature hepatocyte marker genes in d8-HNF4A+ HECs and d28-AAT+ HLCs were affected by addition of DMSO. One exception was the lower levels of active marks in mature hepatocyte gene regulatory regions of DMSO-treated d28-AAT+ cells. However, we observed higher POL2RA levels and lower total H3 levels in nearly all gene promoters and enhancers. Although we cannot formally exclude the possibility that some loci, particularly during early differentiation, are sensitive to global or local alteration of acetylation, this observation may suggest that DMSO affects differentiation in general by altering chromatin accessibility in a more global fashion, as suggested by Lapeyre and co-workers (Lapeyre and Bekhoe, 1974; Stratling, 1976).

EZH2 Inhibition Does Not Improve In Vitro Hepatocyte Differentiation from hESCs

As we consistently found high levels of H3K27me3 at promoters and enhancers of d28-AAT+ cells compared with PHHs (Figures 2A–2E), we hypothesized that removal of H3K27me3 might allow maturation of HLCs to a more mature PHH phenotype. As EZH2 is the histone methyltransferase that catalyzes H3K27 trimethylation (Figure 5A) (Verma et al., 2012), we supplemented the culture medium with an inhibitor against EZH2 (GSK-343, hereafter EZH2i) to reduce H3K27me3 levels, between days 6 and 16 when levels of H3K27me3 marks at marker gene promoters and enhancers increased (Figures 5B, 2A–2E, and S2C). An additional rationale to explore the role of EZH2 was provided by the observation that EZH2 transcripts were higher in d28-AAT+ HLCs compared with PHHs (Figure S5A).

We reassessed transcripts for mature hepatocyte marker genes and the histone profiles at both regulatory regions of these genes in FACS-sorted AAT+ cells on day 28 (Figure 5B). Addition of EZH2i to the differentiating hESCs resulted in a global reduction of H3K27me3. This effect was not further enhanced by a combination treatment of EZH2i and DMSO, a known HDAC inhibitor (Figure 5C). ChIP-qPCR analysis of EZH2i-treated d28-AAT+ cells revealed a >50% reduction in H3K27me3 at both regulatory regions of OCT4, HNF4A, AFP, ALB, AAT, and CYP3A4 (Figure 5D). H3K4me3 enrichment appeared to be increased overall upon combined EZH2i/DMSO treatment (Figure S5B). However, the 50% reduction of H3K27me3 did not result in a significant increase of mature hepatic marker transcripts in the d28-AAT+ cells, regardless of the differentiation protocol (Figure 5E). In line with the qRT-PCR results, addition of EZH2i (in both differentiation protocols) did not increase the fraction of AAT+ or HNF4A+ cells (Figures 5F and 5G) on day 28. Thus, reducing H3K27me3 by 50% at both regulatory regions of mature hepatocyte marker genes by EZH2 inhibition did not improve the maturation of AAT+ HLCs.

DISCUSSION

hPSC-derived hepatocytes are an attractive, alternative cell system for PHHs to test the safety, efficacy, and metabolization of new chemical entities. However, to date most hPSC differentiation protocols yield cells with phenotypic characteristics of fetal rather than mature hepatocytes. Multiple studies demonstrated that hPSC-derived hepatocytes show inferior drug-metabolizing enzyme activity/expression (e.g., CYP3A4 and CYP2A6), and lower levels of transporter proteins (e.g., NTCP or MRP2), and continue to express AFP, a typical fetal hepatocyte marker (Baxter et al., 2015; Chen et al., 2012; Godoy et al., 2015; Hannan et al., 2013; Shan et al., 2013; Siller et al., 2015; Ulvestad et al., 2013). Consistently, we found that d28-hESC progeny continue to express AFP, and that transcripts for numerous primary hepatocyte TFs and functional genes were at significantly lower levels in d28-hESC progeny than in PHHs. Likewise, mRNA levels of some TFs and functional genes were also lower than in hepatocytes from embryos between 20 and 38 weeks.

As epigenetic regulatory mechanisms control DNA-templated activities, including gene transcription, we hypothesized that evaluating the nature and dynamics of

Figure 4. Chromatin Modifications at Promoters and Enhancers of FACS-Sorted HNF4A+ and AAT+ Cells Treated with or without DMSO

(A and C) Relative gene expression (to GAPDH) of pluripotent and hepatic marker genes in d8-HNF4A+ cells (A) and d28-AAT+ cells (C) from cultures with (white) or without (black) DMSO. Data represent mean ± SEM of n = 3 independent experiments.

(B and D) Enrichment of H3K4me3/me2/me1, H3K27ac and H3K27me3, and POL2RA at promoters (left panels) and enhancers (right panels) of OCT4, HNF4A, AFP, ALB, AAT, and CYP3A4 genes in d8-HNF4A+ cells (B) and d28-AAT+ cells (D) treated either without (HNF4A+/AAT+ −DMSO, black) or with DMSO (HNF4A+/AAT+ +DMSO, white). Note that HNF4A+ −DMSO and AAT+ −DMSO data represented in these graphs are identical to the HNF4A+ and AAT+ data in Figure 2. Data represent mean ± SD of n ≥ 2 independent experiments. See also Figure S4.
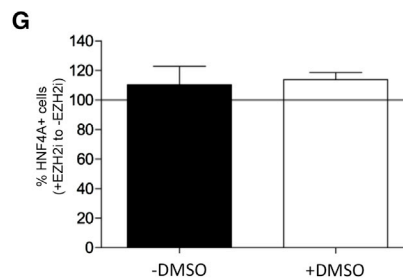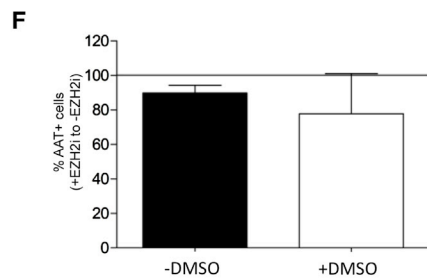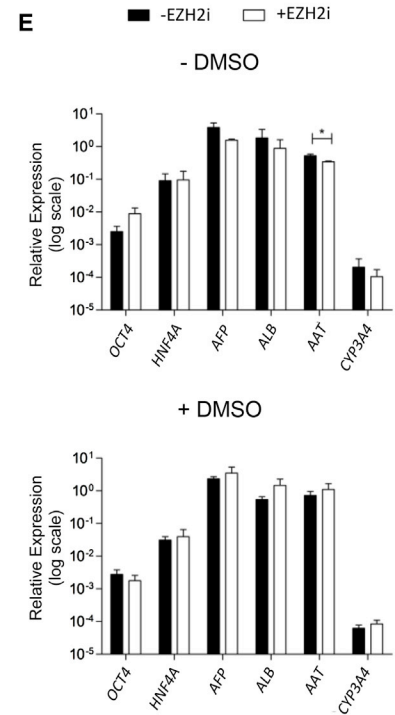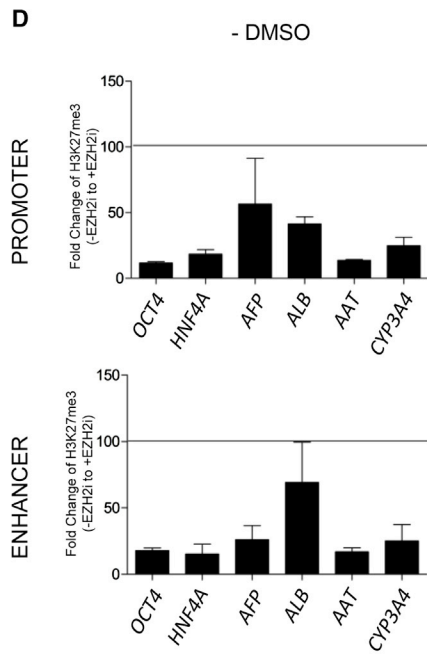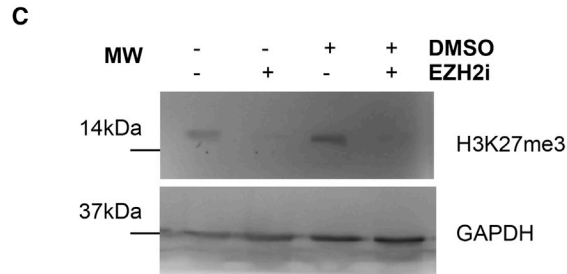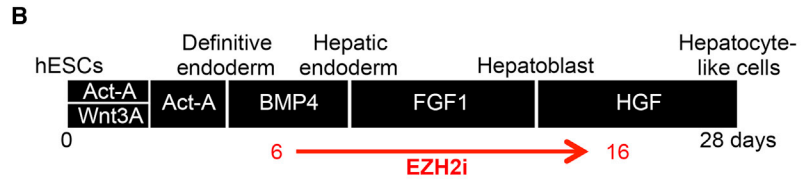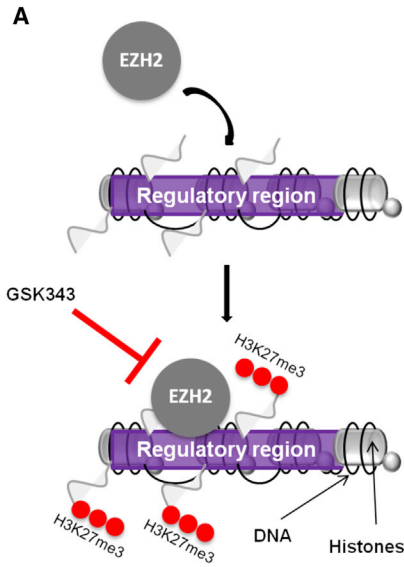
(legend on next page)

epigenetic changes at gene regulatory regions during hepatocyte commitment of hESCs and comparing differences between HLCs and PHHs might identify important hurdles to be overcome to generate more mature hepatocytes from PSCs. Therefore, we investigated histone marking at gene promoters and enhancers of a number of key genes expressed during hepatocyte differentiation. To avoid assessing histone marks in mixed hESC progeny, we isolated pure fractions of d8-HNF4A+ and d28-AAT+ cells.

In accordance with an earlier report, histone marks associated with transcriptional activity at the promoters of the *HNF4A* and *AFP* genes in d8-HNF4A+ cells correlated with the gene transcriptional status (Kim et al., 2011). We further demonstrated that this correlation was also true for the enhancers. In addition, active H3K4me2/me3 and H3K27ac at *ALB* and *AAT* gene promoters and enhancers clearly coincided with increased expression of these genes between days 8 and 28. Surprisingly, we observed that H3K27me3 at promoters and enhancers of hepatoblast/hepatocyte marker genes were significantly higher in d28-AAT+ HLCs than in d8-HNF4A+ HECs, even though transcript levels for these genes increased significantly by day 28, even if they remained significantly lower than in PHHs. These results contradict earlier published results (Kim et al., 2011). A recent study on in vivo endocrine progenitor development also demonstrated gain of H3K27me3 at regulatory regions of genes involved in differentiation and morphogenesis (Xu et al., 2014).

Persistent marking of regulatory gene regions by H3K27me3 despite increased gene transcription supports the notion that H3K27me3 might not be the only determinant of gene activity. A similar finding has been reported recently in the context of transcriptional activation of the immediate-early gene *ATF3*, in response to serum stimulation: ATF3 induction occurred in the presence of the presumed repressive H3K27me3 and did not require removal of the mark (Prickaerts et al., 2012).

We also compared histone modifications in d28-AAT+ HLCs with those in uncultured PHHs to determine whether specific epigenetic marks might be responsible for the incomplete maturation of HLCs. This revealed that active marks in hepatocyte marker gene promoters and enhancers were similar in d28-AAT+ HLCs and PHHs, while H3K27me3 marks were significantly higher in d28-AAT+ cells compared with PHHs. This suggested that H3K27me3 marking in part explains the apparent inability to generate fully mature hepatocytes from hESCs.

Multiple studies have used DMSO to improve or maintain hepatocyte maturity, by for instance maintaining or increasing expression of nuclear receptors, hepatocyte-specific TFs, and drug-metabolizing enzymes (Kanebratt and Andersson, 2008; Nishimura et al., 2003; Su and Waxman, 2004). Therefore, DMSO has been included in hPSC hepatocyte differentiation cultures (Basma et al., 2009; Czysz et al., 2015; Duan et al., 2010; Hay et al., 2008; Kondo et al., 2014; Szkolnicka et al., 2014; Ulvestad et al., 2013). As DMSO appears to improve PSC-hepatocyte differentiation, we repeated the differentiation protocol in the presence of 0.6% DMSO. DMSO generated, in a much more robust way, definitive endoderm as was reported before (Chetty et al., 2013). This was associated with a significantly more homogeneous population of d28-HLCs. However, stage-specific transcripts for hepatic endoderm markers in d8-HNF4A+ cells and hepatocyte markers in d28-AAT+ sorted cells from cultures with or without DMSO were not significant different, and transcripts in d28-AAT+ cells from DMSO-containing cultures remained significantly lower than in PHHs. H3K27me3 at hepatoblast/hepatocyte marker gene promoters and enhancers were also not reduced in response to DMSO in d8-HNF4A+ cells and d28-AAT+ cells. Consistent with the function of DMSO as an HDAC, H3K27ac marks at the enhancers of marker genes were increased.

Fetal hepatocyte progenitors express EZH2, the histone lysine methyltransferase responsible for H3K27 trimethylation, and EZH2 is required to allow hepatocyte progenitor

Figure 5. Effect of EZH2 Inhibition on hESC-Derived HLCs Treated with or without DMSO on H3K27me3 Enrichment, Protein, and Transcript Levels

(A) Schematic overview of EZH2 function and effect of GSK-343.

(B) Schematic overview of hepatocyte differentiation protocol with the time frame (days 6–16) in which 1 μM GSK-343 (referred to as EZH2 inhibitor [EZH2i]) was added.

(C) Western blot for H3K27me3 in FACS-sorted AAT+ cells at day 28 obtained by both differentiation protocols in the presence or absence of the EZH2i. The molecular weight size marker was cropped from the gel.

(D) Graphs represent fold change enrichment of H3K27me3 at promoters and enhancers *OCT4* and hepatic markers in EZH2i-treated (black bars) compared with non-treated cells (line) in both d28-AAT+ sorted cells with or without DMSO.

(E) Relative gene expression (to *GAPDH*) profile of *OCT4* and hepatic markers in both differentiation protocols treated with (white) or without (black) EZH2i.

(F and G) Percent AAT+ cells (by FACS) (F) and percent HNF4A+ cells (by ICC) (G) in EZH2i-treated (bars) compared with non-treated cells (line) in d28 progeny with or without DMSO.

Data, except for (C), represent mean ± SEM of n = 3 independent experiments. *p < 0.05 by Student's t test. See also Figure S5.

expansion in vivo (Koike et al., 2014). Conversely, knockdown of EZH2 in embryonic murine hepatic progenitors was reported to promote their differentiation to hepatocytes, with an upregulation of several transcriptional regulators of hepatocyte differentiation (Aoki et al., 2010). Similar findings have also been published for endocrine pancreas differentiation (Aoki et al., 2010; Xu et al., 2014). Differentiation of endocrine pancreatic cells to mature β cells in vitro becomes possible after grafting the cells in vivo, and this is associated with complete removal of Polycomb group-mediated repression at stage-specific genes (Xie et al., 2013a). As EZH2 levels were significantly higher in d28-AAT$^+$ cells than in PHHs, we tested whether inhibition of EZH2 would allow further HLC maturation via reduction of H3K27me3. Even if inhibition of EZH2 reduced H3K27me3 at both regulatory regions of hepatocyte genes by 50%, gene expression and protein levels of mature hepatocyte markers did not change. It is thus possible that removing only 50% of the H3K27me3 from HLCs is insufficient to allow full maturation to a PHH state. Alternatively, it is also possible that the impact of the repression-associated H3K27me3 marking may be reinforced by other repressive histone modifications in hESC progeny.

In summary, we demonstrate that the in vitro differentiation of hESC-derived cells to hepatocytes is accompanied by dynamic epigenetic regulation. Although hESC-derived HLC promoter and enhancer decoration with active epigenetic marks resembles that in PHHs, repressive H3K27me3 marks at hepatocyte marker gene promoters and enhancers in HLCs did not reflect histone marking observed in uncultured PHHs. Modulation of promoter and enhancer H3K27me3 marking by inhibition of EZH2 activity did not yield enhanced hepatocyte maturation. This suggests that H3K27me3 is not solely responsible for the lack of maturation of ESC progeny, but may be reinforced by other repressive histone modifications. Future studies will be needed to gain insights into the functional links between signaling events in the hepatocyte environment that support the establishment of an epigenetic state more akin to that of PHHs, thus to optimize differentiation protocols aimed at generating functional hepatocytes from hPSCs.

EXPERIMENTAL PROCEDURES

hESC Differentiation to the Hepatocyte Lineage

The hESC H9 line (WAO9, WiCell) was cultured on inactivated mouse embryonic fibroblasts (iMEF) as described by Thomson et al. (1998). Experiments were performed with approval from the Medical Ethics Committee (UZ Leuven, Gasthuisberg). Hepatocyte differentiation was done as described earlier with minor adaptations (Roelandt et al., 2013) (Figure 1A). For the DMSO-treated cell culture condition, cells were supplemented from days 0 to 28

to 0.6% DMSO (Sigma-Aldrich). EZH2 inhibition was induced in the cultures by administration of 1 μM GSK-343 (Sigma-Aldrich, SML0766) from days 6 to 16 by changing media completely every 2 days. All growth factors were purchased from PeproTech.

FACS

Cells were harvested with 0.05% trypsin-EDTA (d8) or liberase (d28) (Roche), fixed with 1% ice-cold formaldehyde (Fluka) for 10 min at room temperature, and quenched with 0.125 mM glycine for 5 min at room temperature. Fixed cells were permeabilized and blocked with 10% goat serum (Dako)/0.1% saponin/PBS for 45 min at room temperature, followed by incubation with 1 μg/ml/10^6 cells anti-HNF4A and anti-AAT primary antibodies (Abs) or isotypes in 1% goat serum/PBS for 1 hr at room temperature (Table S1). Secondary Abs (Alexa Fluor 488 [1:1000], Alexa Fluor 555 [1:1000], or Alexa Fluor 647 [1:1500], Invitrogen) were used for 30 min at room temperature in the dark before sorting the samples on a FACS AriaIII cell sorter (BD Biosciences). Data were analyzed with FACS Diva Software (BD Biosciences). Cells were stored at −80°C.

RNA Extraction from FACS-Sorted Cells

Cells were fixed with 1% ice-cold formaldehyde (Fluka) for 10 min at room temperature, and quenched by adding 0.125 mM glycine for 5 min supplemented with 1:125 RNasin Plus RNase Inhibitor (Promega). All the subsequent steps were carried out as described above under FACS. Cells were washed with PBS containing 1:200 RNasin Plus RNase Inhibitor. RNasin Plus RNase Inhibitor (1:60) was added to the permeabilization/blocking, primary, and secondary solutions. Following secondary Ab staining cells were washed twice in PBS, and resuspended in PBS with 0.5% goat serum and 1:100 RNasin Plus RNase Inhibitor. Cells were sorted on a FACS AriaIII cell sorter (BD Biosciences) and were collected in tubes coated with a small amount of PBS with 0.5% goat serum and 1:100 RNasin Plus RNase Inhibitor. After sorting, cells were recovered by centrifugation at 2,200 × g for 15 min at 4°C. To reverse the formaldehyde crosslinking, cell pellets were incubated in 200 μL of 200 mM NaCl, 10 mM Tris-HCl (pH 8), 1 mM EDTA, 1% SDS, and 1:200 RNasin Plus RNase Inhibitor for 2 hr at 65°C (Jeyapalan and Sedivy, 2013). An equal amount volume of TRIzol reagent (Ambion) was added. RNA was extracted according to the TRIzol manufacturer's instructions.

ICC for Pluripotent and Hepatic Markers

Cells differentiated on glass slides were fixed with 4% paraformaldehyde (PFA) for 15 min at room temperature, permeabilized with 0.2% Triton X-100 in PBS (PBS-T), blocked with 0.2% PBS-T supplemented with 5% normal donkey serum (Jackson Laboratory), and stained overnight at 4°C with OCT4 (0.4 μg/mLl), HNF4A (5 μg/mLl), AFP (4.5 μg/mL), ALB (2.5 μg/mL), AAT (3.95 μg/mL), or the relevant isotype control Abs in Dako diluents (Dako) (Table S1). Immune complexes were detected by incubation with a species-specific AF555-conjugated immunoglobulin G (4 μg/mL, Alexa Fluor, Molecular Probes) for 30 min at room temperature. The nuclei were visualized using Hoechst (Sigma-Aldrich).

Signals were detected with an Axioimager.Z1 microscope (Carl Zeiss) using extended focus computation from z stacks. The

percentage of positive cells on days 0, 4, and 8 was manually counted on five representative 10× images. Differently for AFP, ALB, and AAT on day 28, which were also detected surrounding the cells, the percentage of positive signal was based on surface area measurements using the measurement module software (Carl Zeiss). For all pictures, the percentage of positive cells was contoured above the isotype level and three different differentiations were averaged.

ChIP

ChIP was performed using 3×10^5 or 6×10^5 cells per IP, respectively, for histone modifications (H3K27me3, H3K27ac, and H3K4me3/me2/me1) and POL2RA. IPs were processed as described previously (Pistoni et al., 2010). Dynabeads (Life Technologies) were added and DNA purified using a QIAquick PCR purification kit (Qiagen). Purified DNA was analyzed by qPCR. Identification of promoter and enhancer regions was based on literature research and the Encyclopedia of DNA elements (ENCODE) database, available online. Sequences of the primers and ChIP-grade Abs used for ChIP are listed in Tables S2 and S3. The ChIP-qPCR data were presented as percent input/total H3: for the histone modifications we calculated by $2^{(-(CT \text{ Histone modification} - CT \text{ 10\% input}))}/2^{(-(CT \text{ total H3} - CT \text{ 10\% input}))}$ and for POL2RA we calculated by $2^{(-(CT \text{ POL2RA} - CT \text{ 10\% input}))}$.

Statistical Analysis

Comparisons between two data groups (with n ≥ 3 independent experiments) were analyzed using an unpaired two-tailed Student's t test (GraphPad Prism 5) (De winter, 2013). p Values of less than 0.05 were considered significant and are indicated in the graphs as *p < 0.05, **p < 0.01, or ***p < 0.001. All data represent the mean ± SEM (n ≥ 3) or mean ± SD (n = 2). To investigate the relationship between cell population (d8-HNF4A+ versus d8-HNF4A− cells and d28-AAT+ cells versus PHHs) and histone enrichment via gene expression levels, a mediation analysis was performed (Krull and MacKinnon, 1999). This involved a regression of gene expression level on cell population, and regression models of each histone modification on gene expression levels. In all models, gene was used as a repeated measure to obtain relationships averaged over all genes, and gene and histone levels were log transformed due to heavy skewness. The indirect effect of cell population on gene expression for each histone modification was then obtained by combining the models using the Sobel method (Krull and MacKinnon, 1999).

SUPPLEMENTAL INFORMATION

Supplemental Information includes Supplemental Experimental Procedures, five figures, and three tables and can be found with this article online at http://dx.doi.org/10.1016/j.stemcr.2016.06.013.

AUTHOR CONTRIBUTIONS

J.V., M.P., and C.M.V. conceived, designed, and planned the study, generated the data, interpreted the experiments, and wrote the manuscript. M.W. contributed to the maintenance of the hepatic differentiation cultures and analysis of the epigenetic and gene expression profiles. K.E. and V.S. contributed to the immunocytochemical characterization of the differentiation. N.H. contributed to the optimization of differentiation protocol with DMSO. R.B. helped with the interpretation of data. M.N. and E.S. performed the isolation and characterization of the human hepatocyte samples. P.C and J.W.V. provided scientific discussions, helped with data interpretation, and contributed to writing the manuscript. All of the authors have read and edited the manuscript.

ACKNOWLEDGMENTS

REFERENCES

Aoki, R., Chiba, T., Miyagi, S., Negishi, M., Konuma, T., Taniguchi, H., Ogawa, M., Yokosuka, O., and Iwama, A. (2010). The polycomb group gene product Ezh2 regulates proliferation and differentiation of murine hepatic stem/progenitor cells. J. Hepatol. 52, 854–863.

Azuara, V., Perry, P., Sauer, S., Spivakov, M., Jorgensen, H.F., John, R.M., Gouti, M., Casanova, M., Warnes, G., Merkenschlager, M., et al. (2006). Chromatin signatures of pluripotent cell lines. Nat. Cell Biol. 8, 532–538.

Bannister, A.J., and Kouzarides, T. (2011). Regulation of chromatin by histone modifications. Cell Res. 21, 381–395.

Basma, H., Soto-Gutierrez, A., Yannam, G.R., Liu, L., Ito, R., Yamamoto, T., Ellis, E., Carson, S.D., Sato, S., Chen, Y., et al. (2009). Differentiation and transplantation of human embryonic stem cell-derived hepatocytes. Gastroenterology 136, 990–999.

Baxter, M.A., Rowe, C., Alder, J., Harrison, S., Hanley, K.P., Park, B.K., Kitteringham, N.R., Goldring, C.E., and Hanley, N.A. (2010). Generating hepatic cell lineages from pluripotent stem cells for drug toxicity screening. Stem Cell Res. 5, 4–22.

Baxter, M., Withey, S., Harrison, S., Segeritz, C.P., Zhang, F., Atkinson-Dell, R., Rowe, C., Gerrard, D.T., Sison-Young, R., Jenkins, R., et al. (2015). Phenotypic and functional analyses show stem cell-derived hepatocyte-like cells better mimic fetal rather than adult hepatocytes. J. Hepatol. 62, 581–589.

Bernstein, B.E., Mikkelsen, T.S., Xie, X., Kamal, M., Huebert, D.J., Cuff, J., Fry, B., Meissner, A., Wernig, M., Plath, K., et al. (2006). A bivalent chromatin structure marks key developmental genes in embryonic stem cells. Cell *125*, 315–326.

Boland, M.J., Nazor, K.L., and Loring, J.F. (2014). Epigenetic regulation of pluripotency and differentiation. Circ. Res. *115*, 311–324.

Calo, E., and Wysocka, J. (2013). Modification of enhancer chromatin: what, how, and why? Mol. Cell *49*, 825–837.

Chen, Y.F., Tseng, C.Y., Wang, H.W., Kuo, H.C., Yang, V.W., and Lee, O.K. (2012). Rapid generation of mature hepatocyte-like cells from human induced pluripotent stem cells by an efficient three-step protocol. Hepatology *55*, 1193–1203.

Chetty, S., Pagliuca, F.W., Honore, C., Kweudjeu, A., Rezania, A., and Melton, D.A. (2013). A simple tool to improve pluripotent stem cell differentiation. Nat. Methods *10*, 553–556.

Creyghton, M.P., Cheng, A.W., Welstead, G.G., Kooistra, T., Carey, B.W., Steine, E.J., Hanna, J., Lodato, M.A., Frampton, G.M., Sharp, P.A., et al. (2010). Histone H3K27ac separates active from poised enhancers and predicts developmental state. Proc. Natl. Acad. Sci. USA *107*, 21931–21936.

Czysz, K., Minger, S., and Thomas, N. (2015). DMSO efficiently down regulates pluripotency genes in human embryonic stem cells during definitive endoderm derivation and increases the proficiency of hepatic differentiation. PLoS One *10*, e0117689.

De winter, J.C.F. (2013). Using the Student's t-test with extremely small sample sizes. Pract. Assess. Res. Eval. *18*. http://pareonline.net/getvn.asp?v=18&n=10.

Duan, Y., Ma, X., Zou, W., Wang, C., Bahbahan, I.S., Ahuja, T.P., Tolstikov, V., and Zern, M.A. (2010). Differentiation and characterization of metabolically functioning hepatocytes from human embryonic stem cells. Stem Cells *28*, 674–686.

Godoy, P., Schmidt-Heck, W., Natarajan, K., Lucendo-Villarin, B., Szkolnicka, D., Asplund, A., Bjorquist, P., Widera, A., Stober, R., Campos, G., et al. (2015). Gene networks and transcription factor motifs defining the differentiation of stem cells into hepatocyte-like cells. J. Hepatol. *63*, 934–942.

Guenther, M.G., Levine, S.S., Boyer, L.A., Jaenisch, R., and Young, R.A. (2007). A chromatin landmark and transcription initiation at most promoters in human cells. Cell *130*, 77–88.

Hannan, N.R., Segeritz, C.P., Touboul, T., and Vallier, L. (2013). Production of hepatocyte-like cells from human pluripotent stem cells. Nat. Protoc. *8*, 430–437.

Harshman, S.W., Young, N.L., Parthun, M.R., and Freitas, M.A. (2013). H1 histones: current perspectives and challenges. Nucleic Acids Res. *41*, 9593–9609.

Hay, D.C., Zhao, D., Fletcher, J., Hewitt, Z.A., McLean, D., Urruticoechea-Uriguen, A., Black, J.R., Elcombe, C., Ross, J.A., Wolf, R., et al. (2008). Efficient differentiation of hepatocytes from human embryonic stem cells exhibiting markers recapitulating liver development in vivo. Stem Cells *26*, 894–902.

Heintzman, N.D., Stuart, R.K., Hon, G., Fu, Y., Ching, C.W., Hawkins, R.D., Barrera, L.O., Van Calcar, S., Qu, C., Ching, K.A., et al. (2007). Distinct and predictive chromatin signatures of transcriptional promoters and enhancers in the human genome. Nat. Genet. *39*, 311–318.

Heintzman, N.D., Hon, G.C., Hawkins, R.D., Kheradpour, P., Stark, A., Harp, L.F., Ye, Z., Lee, L.K., Stuart, R.K., Ching, C.W., et al. (2009). Histone modifications at human enhancers reflect global cell-type-specific gene expression. Nature *459*, 108–112.

Helsen, N., Debing, Y., Paeshuyse, J., Dallmeier, K., Boon, R., Coll, M., Sancho-Bru, P., Claes, C., Neyts, J., and Verfaillie, C.M. (2016). Stem cell-derived hepatocytes: a novel model for hepatitis E virus replication. J. Hepatol. *64*, 565–573.

Jeyapalan, J.C., and Sedivy, J.M. (2013). How to measure RNA expression in rare senescent cells expressing any specific protein such as p16Ink4a. Aging (Albany NY) *5*, 120–129.

Kanebratt, K.P., and Andersson, T.B. (2008). Evaluation of HepaRG cells as an in vitro model for human drug metabolism studies. Drug Metab. Dispos. *36*, 1444–1452.

Kim, H., Jang, M.J., Kang, M.J., and Han, Y.M. (2011). Epigenetic signatures and temporal expression of lineage-specific genes in hESCs during differentiation to hepatocytes in vitro. Hum. Mol. Genet. *20*, 401–412.

Koike, H., Ouchi, R., Ueno, Y., Nakata, S., Obana, Y., Sekine, K., Zheng, Y.W., Takebe, T., Isono, K., Koseki, H., et al. (2014). Polycomb group protein Ezh2 regulates hepatic progenitor cell proliferation and differentiation in murine embryonic liver. PLoS One *9*, e104776.

Kondo, Y., Iwao, T., Nakamura, K., Sasaki, T., Takahashi, S., Kamada, N., Matsubara, T., Gonzalez, F.J., Akutsu, H., Miyagawa, Y., et al. (2014). An efficient method for differentiation of human induced pluripotent stem cells into hepatocyte-like cells retaining drug metabolizing activity. Drug Metab. Pharmacokinet. *29*, 237–243.

Krull, J.L., and MacKinnon, D.P. (1999). Multilevel mediation modeling in group-based intervention studies. Eval. Rev. *23*, 418–444.

Lam, M.T., Li, W., Rosenfeld, M.G., and Glass, C.K. (2014). Enhancer RNAs and regulated transcriptional programs. Trends Biochem. Sci. *39*, 170–182.

Lapeyre, J.N., and Bekhoe, I. (1974). Effects of 5-bromo-2′-deoxyuridine and dimethyl sulfoxide on properties and structure of chromatin. J. Mol. Biol. *89*, 137–162.

Mann, D.A. (2015). Human induced pluripotent stem cell-derived hepatocytes for toxicology testing. Expert Opin. Drug Metab. Toxicol. *11*, 1–5.

Meissner, A. (2010). Epigenetic modifications in pluripotent and differentiated cells. Nat. Biotechnol. *28*, 1079–1088.

Mikkelsen, T.S., Ku, M., Jaffe, D.B., Issac, B., Lieberman, E., Giannoukos, G., Alvarez, P., Brockman, W., Kim, T.K., Koche, R.P., et al. (2007). Genome-wide maps of chromatin state in pluripotent and lineage-committed cells. Nature *448*, 553–560.

Nishimura, M., Ueda, N., and Naito, S. (2003). Effects of dimethyl sulfoxide on the gene induction of cytochrome P450 isoforms, UGT-dependent glucuronosyl transferase isoforms, and ABCB1 in primary culture of human hepatocytes. Biol. Pharm. Bull. *26*, 1052–1056.

Ong, C.T., and Corces, V.G. (2012). Enhancers: emerging roles in cell fate specification. EMBO Rep. *13*, 423–430.

Pekowska, A., Benoukraf, T., Zacarias-Cabeza, J., Belhocine, M., Koch, F., Holota, H., Imbert, J., Andrau, J.C., Ferrier, P., and Spicuglia, S. (2011). H3K4 tri-methylation provides an epigenetic signature of active enhancers. EMBO J. *30*, 4198–4210.

Pistoni, M., Verrecchia, A., Doni, M., Guccione, E., and Amati, B. (2010). Chromatin association and regulation of rDNA transcription by the Ras-family protein RasL11a. EMBO J. *29*, 1215–1224.

Pokholok, D.K., Harbison, C.T., Levine, S., Cole, M., Hannett, N.M., Lee, T.I., Bell, G.W., Walker, K., Rolfe, P.A., Herbolsheimer, E., et al. (2005). Genome-wide map of nucleosome acetylation and methylation in yeast. Cell *122*, 517–527.

Prickaerts, P., Niessen, H.E., Mouchel-Vielh, E., Dahlmans, V.E., van den Akker, G.G., Geijselaers, C., Adriaens, M.E., Spaapen, F., Takihara, Y., Rapp, U.R., et al. (2012). MK3 controls Polycomb target gene expression via negative feedback on ERK. Epigenetics Chromatin *5*, 12.

Rada-Iglesias, A., Bajpai, R., Swigut, T., Brugmann, S.A., Flynn, R.A., and Wysocka, J. (2011). A unique chromatin signature uncovers early developmental enhancers in humans. Nature *470*, 279–283.

Roelandt, P., Obeid, S., Paeshuyse, J., Vanhove, J., Van Lommel, A., Nahmias, Y., Nevens, F., Neyts, J., and Verfaillie, C.M. (2012). Human pluripotent stem cell-derived hepatocytes support complete replication of hepatitis C virus. J. Hepatol. *57*, 246–251.

Roelandt, P., Vanhove, J., and Verfaillie, C. (2013). Directed differentiation of pluripotent stem cells to functional hepatocytes. Methods Mol. Biol. *997*, 141–147.

Schmelzer, E., Wauthier, E., and Reid, L.M. (2006). The phenotypes of pluripotent human hepatic progenitors. Stem Cells *24*, 1852–1858.

Schneider, R., Bannister, A.J., Myers, F.A., Thorne, A.W., Crane-Robinson, C., and Kouzarides, T. (2004). Histone H3 lysine 4 methylation patterns in higher eukaryotic genes. Nat. Cell Biol. *6*, 73–77.

Schubeler, D., MacAlpine, D.M., Scalzo, D., Wirbelauer, C., Kooperberg, C., van Leeuwen, F., Gottschling, D.E., O'Neill, L.P., Turner, B.M., Delrow, J., et al. (2004). The histone modification pattern of active genes revealed through genome-wide chromatin analysis of a higher eukaryote. Genes Dev. *18*, 1263–1271.

Shan, J., Schwartz, R.E., Ross, N.T., Logan, D.J., Thomas, D., Duncan, S.A., North, T.E., Goessling, W., Carpenter, A.E., and Bhatia, S.N. (2013). Identification of small molecules for human hepatocyte expansion and iPS differentiation. Nat. Chem. Biol. *9*, 514–520.

Siller, R., Greenhough, S., Naumovska, E., and Sullivan, G.J. (2015). Small-molecule-driven hepatocyte differentiation of human pluripotent stem cells. Stem Cell Rep. *4*, 939–952.

Stadler, M.B., Murr, R., Burger, L., Ivanek, R., Lienert, F., Scholer, A., van Nimwegen, E., Wirbelauer, C., Oakeley, E.J., Gaidatzis, D., et al. (2011). DNA-binding factors shape the mouse methylome at distal regulatory regions. Nature *480*, 490–495.

Stratling, W.H. (1976). Stimulation of transcription on chromatin by polar organic compounds. Nucleic Acids Res. *3*, 1203–1213.

Su, T., and Waxman, D.J. (2004). Impact of dimethyl sulfoxide on expression of nuclear receptors and drug-inducible cytochromes P450 in primary rat hepatocytes. Arch. Biochem. Biophys. *424*, 226–234.

Szkolnicka, D., Farnworth, S.L., Lucendo-Villarin, B., and Hay, D.C. (2014). Deriving functional hepatocytes from pluripotent stem cells. Curr. Protoc. Stem Cell Biol. *1*, 1G.5.1–1G.5.12.

Thomson, J.A., Itskovitz-Eldor, J., Shapiro, S.S., Waknitz, M.A., Swiergiel, J.J., Marshall, V.S., and Jones, J.M. (1998). Embryonic stem cell lines derived from human blastocysts. Science *282*, 1145–1147.

Ulvestad, M., Nordell, P., Asplund, A., Rehnström, M., Jacobsson, S., Holmgren, G., Davidson, L., Brolén, G., Edsbagge, J., Björquist, P., et al. (2013). Drug metabolizing enzyme and transporter protein profiles of hepatocytes derived from human embryonic and induced pluripotent stem cells. Biochem. Pharmacol. *86*, 691–702.

Verma, S.K., Tian, X., LaFrance, L.V., Duquenne, C., Suarez, D.P., Newlander, K.A., Romeril, S.P., Burgess, J.L., Grant, S.W., Brackley, J.A., et al. (2012). Identification of potent, selective, cell-active inhibitors of the histone lysine methyltransferase EZH2. ACS Med. Chem. Lett. *3*, 1091–1096.

Visel, A., Blow, M.J., Li, Z., Zhang, T., Akiyama, J.A., Holt, A., Plajzer-Frick, I., Shoukry, M., Wright, C., Chen, F., et al. (2009). ChIP-seq accurately predicts tissue-specific activity of enhancers. Nature *457*, 854–858.

Wamstad, J.A., Alexander, J.M., Truty, R.M., Shrikumar, A., Li, F., Eilertson, K.E., Ding, H., Wylie, J.N., Pico, A.R., Capra, J.A., et al. (2012). Dynamic and coordinated epigenetic regulation of developmental transitions in the cardiac lineage. Cell *151*, 206–220.

Xie, R., Everett, L.J., Lim, H.W., Patel, N.A., Schug, J., Kroon, E., Kelly, O.G., Wang, A., D'Amour, K.A., Robins, A.J., et al. (2013a). Dynamic chromatin remodeling mediated by polycomb proteins orchestrates pancreatic differentiation of human embryonic stem cells. Cell Stem Cell *12*, 224–237.

Xie, W., Schultz, M.D., Lister, R., Hou, Z., Rajagopal, N., Ray, P., Whitaker, J.W., Tian, S., Hawkins, R.D., Leung, D., et al. (2013b). Epigenomic analysis of multilineage differentiation of human embryonic stem cells. Cell *153*, 1134–1148.

Xu, C.R., Li, L.C., Donahue, G., Ying, L., Zhang, Y.W., Gadue, P., and Zaret, K.S. (2014). Dynamics of genomic H3K27me3 domains and role of EZH2 during pancreatic endocrine specification. EMBO J. *33*, 2157–2170.

Zhang, Z., Liu, J., Liu, Y., Li, Z., Gao, W.Q., and He, Z. (2013). Generation, characterization and potential therapeutic applications of mature and functional hepatocytes from stem cells. J. Cell Physiol. *228*, 298–305.

Zhu, Z., and Huangfu, D. (2013). Human pluripotent stem cells: an emerging model in developmental biology. Development *140*, 705–717.